Available online at www.sciencedirect.com
ScienceDirect
Journal of Nuclear Materials 372 (2008) 59–65
journal of nuclear materials
www.elsevier.com/locate/jnucmat

Changes in chemical structure of oxidation reaction layers of Zircaloy-4 and Ti by micro X-ray diffractometry

Yang-Soon Park *, Yeong-Keong Ha, Sun-Ho Han, Kwang-Yong Jee, Won-Ho Kim

Nuclear Chemistry Research Division, Korea Atomic Energy Research Institute, P.O. Box 105, Yuseong, Daejeon 305-600, Republic of Korea

Received 7 June 2006; accepted 23 February 2007

Abstract

A micro X-ray diffractometer with a micrometer sized beam concentrator was developed to investigate the changes in the chemical structures of oxide layers for Zr-based alloys (Zircaloy-4) and Ti metal from the center of the cross section to the surface. Zircaloy-4 and Ti metal were chosen because of their use as a fuel cladding and a heat exchange tubing in a nuclear reactor, respectively. The diffraction patterns were obtained from the cross sectional specimens of the oxidized Zircaloy-4 and Ti metal at 50 μm intervals. For the cross section of Zircaloy-4, Zr metal (hexagonal) was identified in the center, ZrO_{2-x} (hexagonal, about 200 μm in thickness) inside the edge and ZrO_2 (monoclinic, about 400 μm in thickness) at the edge. In the case of Ti metal, Ti metal (hexagonal) was identified in the center, TiO (cubic, about 200 μm in thickness) inside the edge and rutile-TiO_2 (tetragonal, about 230 μm in thickness) at the edge. From this study, it was concluded that the intermediate phase formed between the fuel and the cladding can be identified by the micro-XRD system.

PACS: 81.65.Mq

1. Introduction

Recently, increasing the burn-up and the residence time of a fuel in a nuclear reactor is being considered because of the major advantages in the fuel cycle cost, reactor operation and spent fuel management. The increase of the burn-up produces large amount of fission products and damages fuel rod. Thus, numerous studies have been carried out to analyze the safety of spent fuel at high burn-up. The increase of the burn-up leads to structural changes in the area of a pellet periphery (rim) within a few hundreds of micrometers in thickness. In addition, above a certain burn-up, a fuel-cladding chemical interaction has been reported. To investigate the structural changes in the rim and the interface between the fuel and the cladding, XRD data of the thin regions at intervals less than 50 μm is needed. To achieve this, there are several methods to generate a microbeam such as the grazing incidence mirrors, the diffractive mirrors and the refractive lens [1–13]. Among them, a microbeam concentrator by using a couple of Ni mirrors and a line-type aperture was adopted for our XRD system [14]. To confirm the applicability of this system for the identification of width as small as a few tens of micrometers, oxidized metal specimens of Zr and Ti were measured.

The Zircaloy-4 was chosen because it has been used as a cladding material for an UO_2 fuel because of its good mechanical strength, corrosion resistance and neutron absorption cross section. When the pellet contacts with the cladding, an inside oxidation of the cladding occurs due to an oxygen uptake from the UO_2 pellets and the zirconium metal becomes oxidized, resulting in a thinning of the cladding. The importance of a study on a Zircaloy oxidation at a high temperature should be emphasized in relation with the irradiation performance and safety of fuel pins. The oxidation behavior of zirconium alloys as the cladding materials have been discussed at high temperature [15–20]. A number of papers have been published on the

* Corresponding author. Fax: +82 42 868 8148.
E-mail address: nyspark@kaeri.re.kr (Y.-S. Park).

0022-3115/$ - see front matter © 2007 Elsevier B.V. All rights reserved.
doi:10.1016/j.jnucmat.2007.02.006

outer surface oxidation of a cladding, but not so many studies have been done on the inner surface oxidation.

Ti was chosen as a sample specimen because Ti and its alloys are mainly used as pipeline systems in nuclear reactors due to their excellent corrosion resistance, good mechanical properties and suitable durability characteristics [21–24]. However, in their native form TiO_2 films have poor mechanical properties and they are easily fractured under fretting and sliding wear conditions. Many studies have focused on improving the corrosion resistance of the Ti-based alloys at various temperatures. An inside oxidation of titanium metal occurs due to an oxygen uptake from the air or the water vapor. Increasing the temperature and oxidation time promoted a formation of thick oxide layers and a deeper penetration of the oxygen into the metal [25].

This work was focused on the applicability of a micro-XRD system to the identification of thin layers. The results of its application to two oxidation reaction layers of Zr and Ti were presented.

2. Experimental

2.1. Details of micro X-ray diffractometer

The commercial XRD (D5000, SIEMENS) system with a Cu Kα line filtered through a Ni foil was modified by replacing the normal slit and fixed sample stage with a microbeam concentrator and a micro-sample-positioner as shown in Fig. 1. For the X-ray microbeam alignment, the microbeam concentrator was attached to the tilt stage (tilt adjustment: ±2.5°, sensitivity: 1.25 μrad) along with a vertical translator (travel distance: 6 mm, sensitivity: 0.5 μm, repeatability: 2.5 μm). To provide a spatial resolution of less than 50 μm and to maximize the diffraction intensity, a couple of Ni deposited mirrors and a line type exit slit (4000 μm × 20 μm) was adopted. The resulting projected beam width on the sample surface was 47–50 μm for $\theta > 20°$. The sample holder was equipped with a micro-sample-positioner (travel distance: 12.7 mm, sensitivity: 0.8 μm, repeatability: 2.5 μm) for the translations at 5 μm steps. The measurement was carried out with a scanning step of 0.04° for 40 s per each count. The X-ray beam current was 40 mA at a 40 kV beam generation power.

2.2. Preparation of Zircaloy-4 and titanium specimens

The oxidized sample specimens were prepared from Zircaloy-4 plate (5 × 5 mm) of a 1.6 mm thickness and Ti metal plate (10 × 9 mm) of a 3 mm thickness by a heat treatment in a muffle furnace under an atmospheric condition. Zircaloy-4 plate was heated for 10 min at 1200 °C and that of Ti (99.5%, Nilaco) plate was heated for 30 min at 1100 °C. The oxidized sample specimens were sectioned horizontally, molded by epoxy resin, and then polished with abrasive paper (silicon carbide, grit 2000).

3. Results and discussion

3.1. Determination of the chemical structures for the oxidized Zircaloy-4 specimen

As a cladding material for an UO_2 fuel in the nuclear industry, the Zircaloy-4 has been used because of the advantages of good mechanical strength, corrosion resistance and neutron absorption cross section. Since the free energy of formation of zirconium oxide is very low (<∼−900 kJ/mol) [26], Zr metal easily combines with

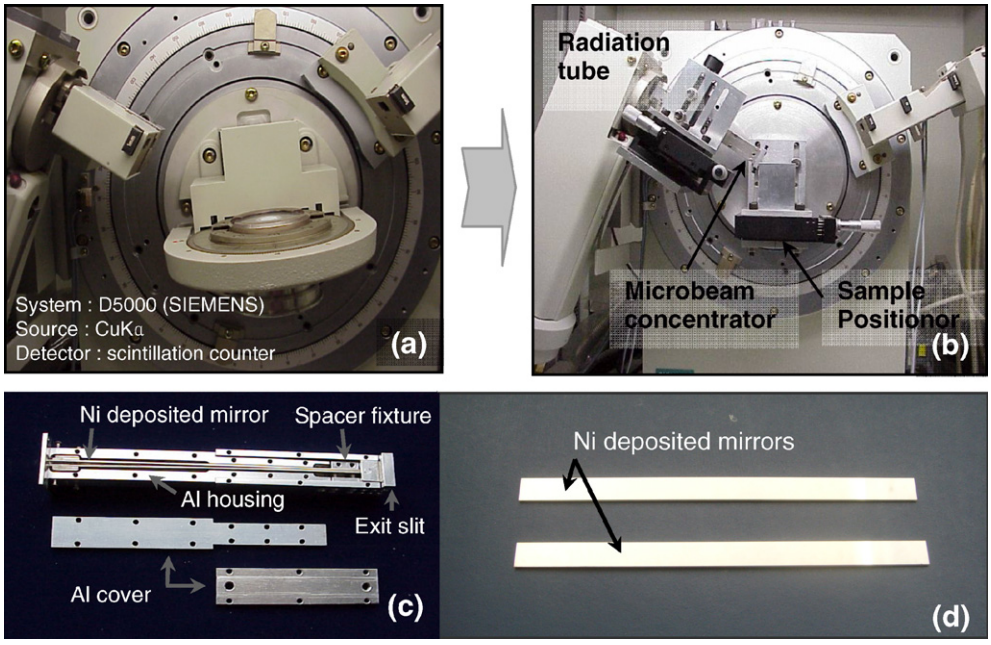

Fig. 1. Conventional X-ray diffractometer (a), micro X-ray diffractometer (b), a concentrator (c) and two Ni deposited mirrors (d) [14].

oxygen and becomes the oxide. The diffusion depth of the oxygen is expanded with the increasing temperatures and the thickness of the zirconium oxide layer is increased [16]. When the burn-up of the fuel is increased or a loss of coolant accident (LOCA) occurs, the temperature of a fuel system rises. At high temperature, the outer surface of a cladding is oxidized by the interaction with the steam and the inner surface is oxidized by the interaction with the oxygen from UO_2 fuel. The inner surface oxidation of a cladding material, one of the modes of the pellet-cladding chemical interaction (PCCI), causes the thinning of a cladding. At temperatures (1200 °C) occurring the rapid oxidation of the Zr metal, a Zircaloy-4 specimen was heated for 10 min and its cross section was measured by a micro-XRD system.

The optical micrograph for the cross sectioned specimen of an oxidized Zircaloy-4 is shown in Fig. 2(A). The edge of the cross section (the dark colored region) represents the oxide layer (about 350 μm in thickness). The inside edge (underneath an oxide layer) shows a bright color and other oxides are expected by the oxygen penetration into a metal in the region. The center shows a metal substrate. Before the oxidation, the thickness of the Zircaloy-4 specimen was 1.6 mm but it became about 2 mm due to its expansion by a thermal oxidation. For the comparison, the cross sectioned specimen was measured by a conventional X-ray diffractometer and the spectrum showed the patterns of ZrO_2 (monoclinic) and ZrO_{2-x} (hexagonal) together (Fig. 3). From this spectrum, ZrO_2 layer cannot be distinguished from the ZrO_{2-x} layer due to the large size of the beam by a normal slit and the fixed sample stage. On the other hand, the XRD patterns of the same specimen measured by the micro-XRD system showed the changes in the chemical structure from the center to the edge of the specimen during an oxidation. Fig. 4 shows the diffraction spectra measured at the edge (a, 200 μm from surface), inside edge (b, 500 μm from surface) and in the center (c, 800 μm from surface) of the cross sectioned specimen of the oxidized Zircaloy-4 in the scanning range of $27° < 2\theta < 40°$. The positions measured by the micro-XRD system are shown as (a), (b) and (c) in Fig. 2(A). Pure zirconium (hexagonal) remained without an oxidation in the center of the cross sectioned specimen (Fig. 4(c)), and the peak shift towards the lower angle was observed in the specimen underneath an external ZrO_2 phase (Fig. 4b), indicating the formation of ZrO_{2-x} (hexagonal)

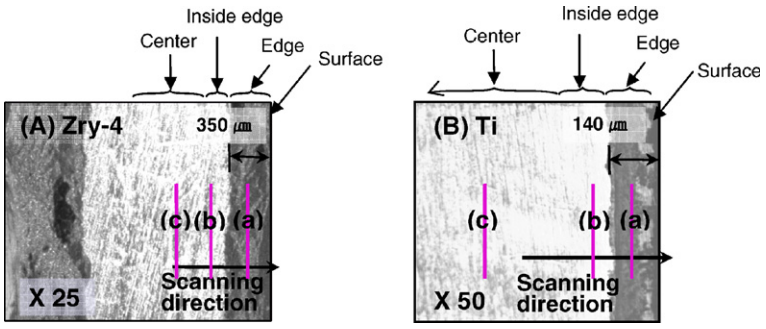

Fig. 2. Optical micrographs of the cross section of the oxidized Zircaloy-4 specimen (A) and the oxidized titanium specimen (B). Edge is an oxide layer with dark color; inside edge is a region with bright color underneath an oxide layer; center is a metal substrate.

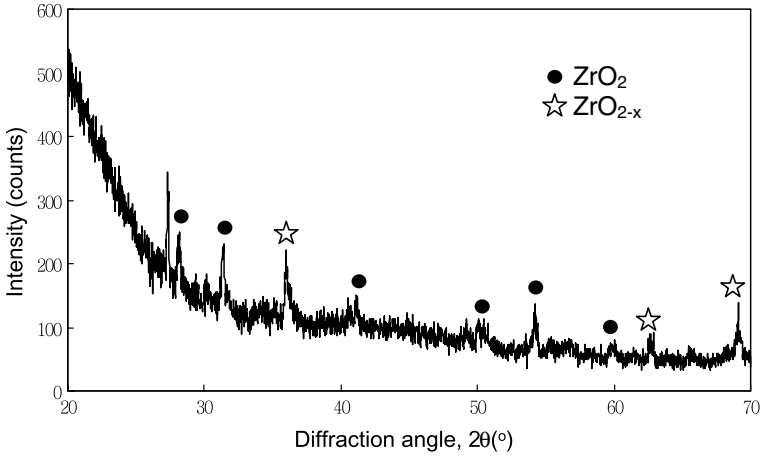

Fig. 3. X-ray diffraction pattern for the cross sectioned oxidized Zircaloy-4 specimen by a conventional X-ray diffractometer. A measuring time/step was 5 s/0.02°.

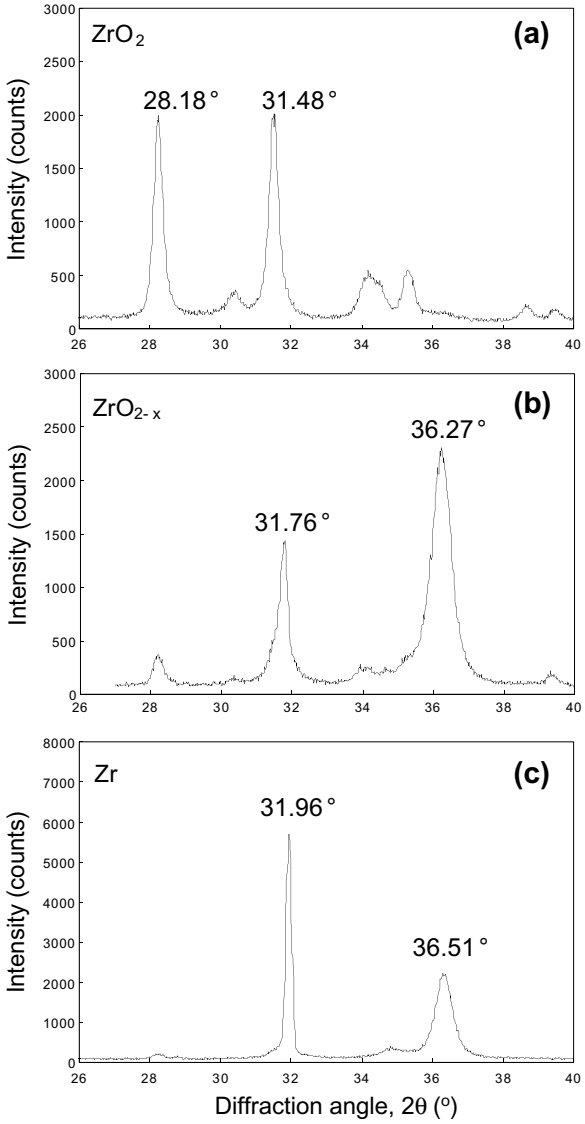

Fig. 4. X-ray diffraction patterns for the cross section of the oxidized Zircaloy-4 specimen by a micro X-ray diffractometer. (a) At the edge, about 200 μm from surface; (b) inside the edge, about 500 μm from surface; (c) in the center, about 800 μm from surface. Refer to Fig. 2(A).

by an incorporation of the oxygen atoms into the Zr structure without the change of a crystal phase. It is known that the stable solid phases of zirconium dissolve oxygen interstitially into their octahedral interstitial sites of hcp metal lattice [27]. At the edge of the specimen, a zirconium dioxide phase of monoclinic was observed. ZrO_2 has three oxide phases of monoclinic ($T_{trs} = 1205$ °C. T_{trs} is defined as transition temperature), tetragonal ($T_{trs} = 1402$ °C) and cubic ($T_{trs} = 2357$ °C) [26]. Among the three phases, it is known that monoclinic-ZrO_2 is the most stable one.

The X-ray spectra measured from the center to the edge of the oxidized specimen at 50 μm intervals are shown in Fig. 5, and the peak intensity of each phase from the core to edge is shown in Fig. 6. Zr phase was observed at the center of the specimen and its peak intensity was decreased gradually from the center to the edge. On the other hand, ZrO_{2-x} phase began to appear underneath an external ZrO_2 phase and it gradually increased up to a maximum, and then it gradually decreased to the edge. ZrO_2 phase was observed near the edge and its intensity was gradually increased to a maximum near the surface and then it was gradually decreased out of the surface (about 800 μm from center).

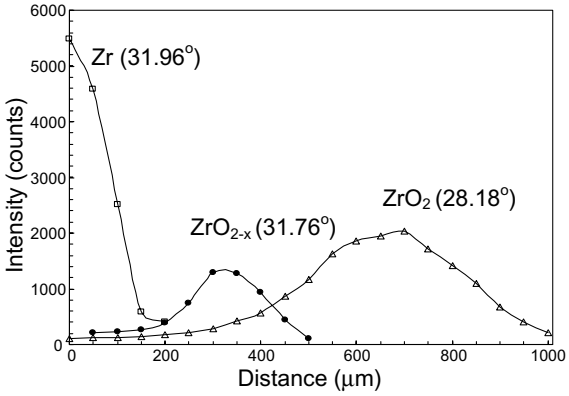

Fig. 6. X-ray diffraction peak intensity at various distances for the oxidized Zircaloy-4 specimen.

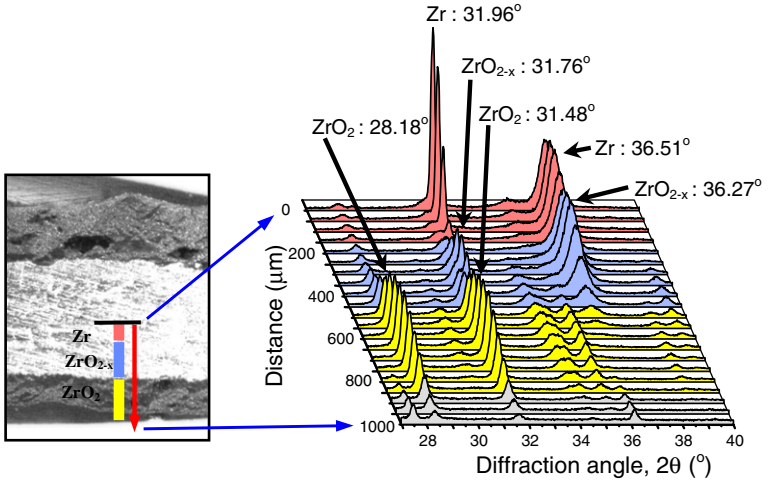

Fig. 5. The variation of the XRD patterns at various distances for the oxidized Zircaloy-4 specimen measured by micro-XRD.

The thickness of ZrO_{2-x} layer (hexagonal) inside edge seems to be a half of the thickness of ZrO_2 layer (monoclinic, about 400 μm) at the edge. As discussed above, this system can provide information not only about the chemical structure but also about the thickness of individual layers.

3.2. Determination of the chemical structures for the oxidized titanium specimen

X-ray diffraction spectrum of a pure titanium metal showed a hexagonal crystal structure before the oxidation (Fig. 7(b)). When the titanium metal was oxidized at 1100 °C, its surface was changed to rutile-TiO_2 (Fig. 7(a)). As shown in Fig. 7(a), the TiO_2 (1 1 0) peak was clearly detected. This phenomenon is ascribed as a result of the orientation of the titanium oxide at a high temperature. High temperature oxidation ($\geqslant$900 °C) promotes the formation of rutile (1 1 0) plane on Ti metal because of surface free energy effect [28]. Though the depth of the penetration of the X-ray is about 7–35 μm, the X-ray diffraction pattern of Ti, base metal inside the TiO_2 layer, was not detected. It means that TiO_2 layer is thicker than the thickness of penetration of X-ray.

The optical micrograph for the cross section of the oxidized titanium specimen is shown in Fig. 2(B). The dark colored region represents the oxide layers (about 140 μm in thickness). For the comparison, the cross sectional specimen was measured by a conventional X-ray diffractometer with a normal slit and the spectrum showed the patterns of rutile-TiO_2 (tetragonal) and Ti (hexagonal) together (Fig. 8). From this spectrum, the other structures were

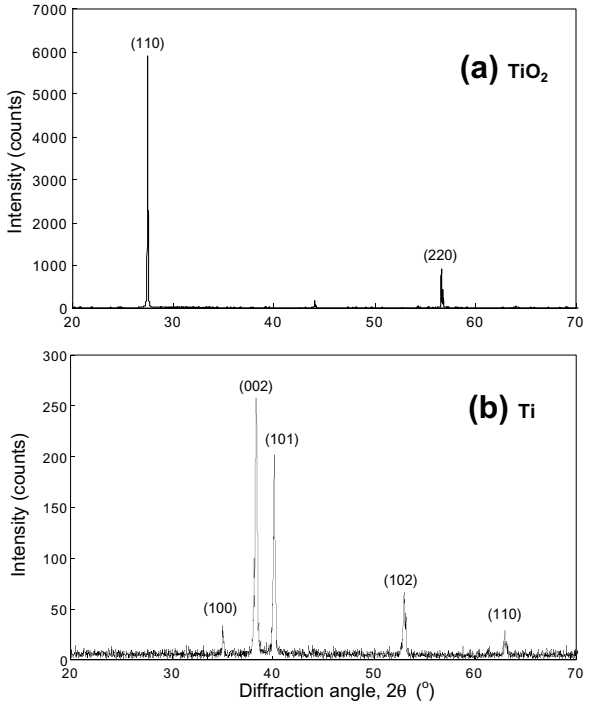

Fig. 7. X-ray diffraction spectra for the surfaces of the Ti specimens by a conventional X-ray diffractometer; (a) after oxidation at 1100 °C in the atmospheric condition; (b) before oxidation.

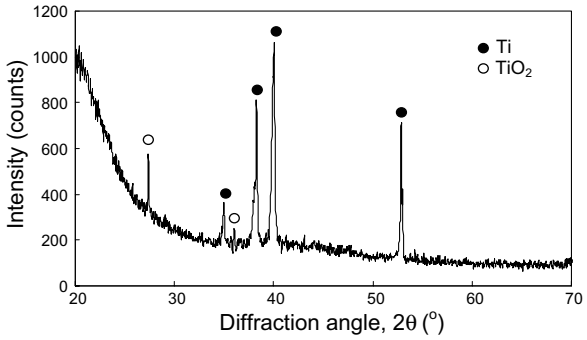

Fig. 8. X-ray diffraction pattern of the cross section of the oxidized titanium specimen by a conventional X-ray diffractometer.

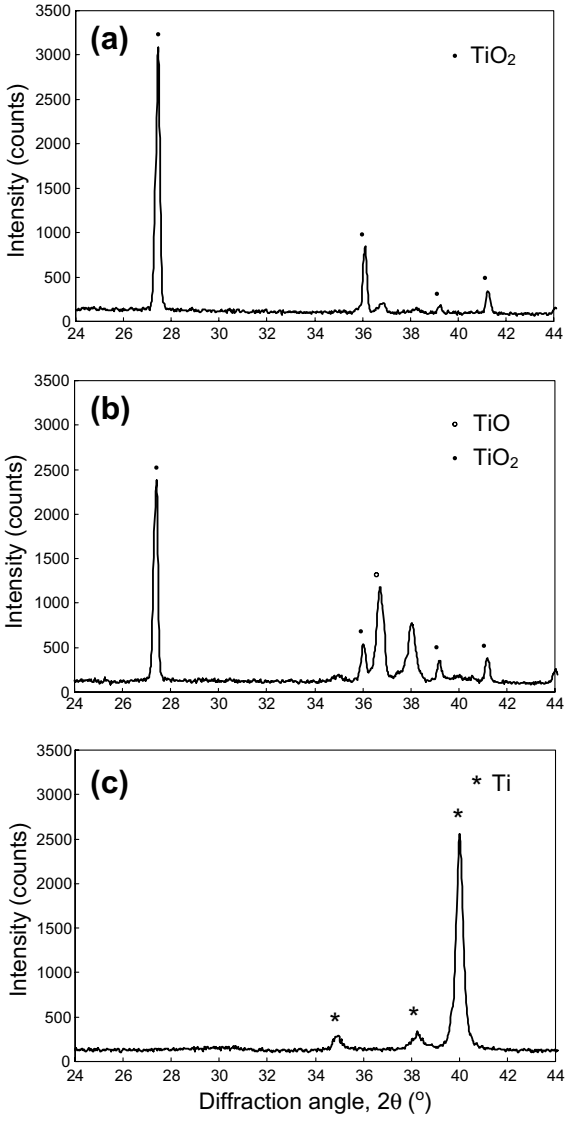

Fig. 9. X-ray diffraction patterns of the oxidized titanium specimen by a micro X-ray diffractometer. (a) At the edge, about 70 μm from surface; (b) inside the edge, about 200 μm from surface; (c) in the center, about 600 μm from surface. Refer to Fig. 2(B).

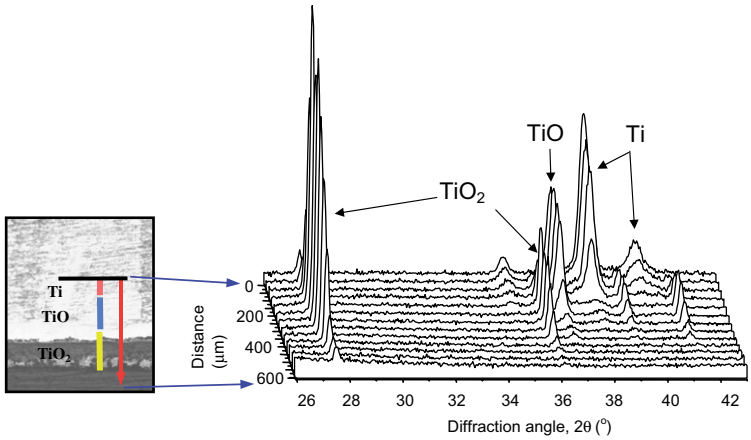

Fig. 10. X-ray diffraction patterns at various distances from the center to the edge of the oxidized titanium specimen.

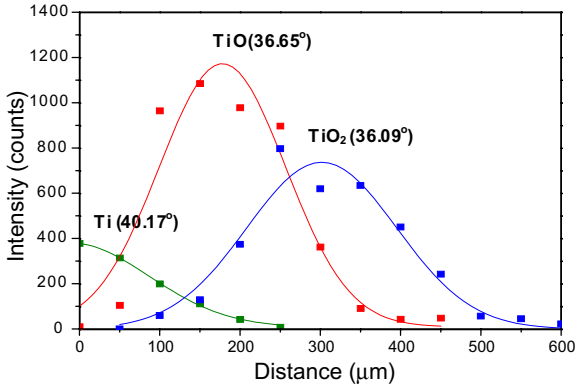

Fig. 11. X-ray diffraction peak intensity at various distances for the oxidized titanium specimen.

not detected. However, many researchers have reported a resultant TiO_{2-x} (Ti_3O_5, Ti_2O_3, TiO, Ti_2O, etc.) by an inside oxidation of Ti metal [21–23,27–29]. The XRD patterns of the same specimen measured by the micro-XRD system showed the changes in the chemical structure from the center to the edge of the specimen during an oxidation. Fig. 9 shows the diffraction spectra measured at the edge (a, about 70 μm from surface), inside edge (b, about 200 μm from surface) and in the center (c, about 600 μm from surface) of the oxidized titanium specimen in the scanning range of $24° < 2\theta < 44°$. The positions measured by the micro-XRD system are shown as (a), (b) and (c) in Fig. 2(B). Pure titanium (hexagonal) remained without an oxidation in the center of the specimen (Fig. 9(c)). Inside the edge of the specimen, TiO (cubic) and TiO_2 (tetragonal) were observed (Fig. 9(b)). At the edge of the specimen, TiO_2 (tetragonal) was observed (Fig. 9(a)). It is known that the thermal oxidation process of titanium is an oxygen diffusion controlled mechanism. Initially, an oxygen adsorption on titanium surface causes the formation of lower oxides after subsequently, oxygen molecules diffuse through the oxide layer into Ti metal [29]. The X-ray spectra measured from the center to the edge of the oxidized specimen at 50 μm intervals are shown in Fig. 10, and the peak intensity of each phase from the core to the edge is shown in Fig. 11. Ti phase was observed at the center of the specimen and its peak intensity was decreased gradually from the center to the edge. On the other hand, the TiO phase began to appear underneath an external TiO_2 phase and it gradually increased up to a maximum, and then it gradually decreased to the edge. TiO_2 phase was observed near the edge and its intensity was gradually increased to a maximum near the surface and then it was gradually decreased out of the surface (about 400 μm from center). The thickness of the rutile-TiO_2 layer (about 230 μm) at the edge seems to be similar to the thickness of the TiO layer (about 200 μm) inside the edge.

4. Conclusion

A micro X-ray diffractometer with a microbeam concentrator and a micro-sample-positioner was developed to investigate the changes in the chemical structure of the oxide layers for Zircaloy-4 and Ti metal from the center to the edge of the specimen. The diffraction patterns were obtained from the oxidized sample specimens at 50 μm intervals. For Zircaloy-4, Zr metal (hexagonal) was identified in the center, ZrO_{2-x} (hexagonal, about 200 μm in thickness) inside the edge and ZrO_2 (monoclinic, about 400 μm in thickness) at the edge. In the case of the Ti metal, Ti metal (hexagonal) was identified in the center, TiO (cubic, about 200 μm in thickness) inside the edge and rutile-TiO_2 (tetragonal, about 230 μm in thickness) at the edge. As mentioned above, this system can provide information not only about the chemical structure but also about the thickness of individual layers.

From this study, it was concluded that the intermediate phase formed between a fuel and a cladding can be identified by the micro-XRD system which was developed in our laboratory.

And, this technique can be applied to investigate the structural change from core to surface in high burn-up fuel and the oxidation behaviors of various claddings.

Acknowledgement

This work was performed under the Nuclear R&D Programs sponsored by the Ministry of Science and Technology of Korea.

References

[1] D. Papaioannou, J. Spino, Rev. Sci. Instrum. 73 (2002) 2659.
[2] D.H. Bilderback, D.J. Thiel, Rev. Sci. Instrum. 66 (1995) 2059.
[3] Y. Suzuki, F. Uchida, Rev. Sci. Instrum. 63 (1992) 578.
[4] M.R. Howells et al., Opt. Eng. 39 (2000) 2748.
[5] A. Takeuchi, Y. Suzuki, K. Uesugi, S. Aoki, Nucl. Instrum. and Meth. A 467&468 (2001) 302.
[6] S. Hayakawa, A. Iida, S. Aoki, Y. Gohshi, Rev. Sci. Instrum. 60 (1989) 2452.
[7] H.N. Chapman, K.A. Nugent, S.W. Wilkins, Appl. Opt. 32 (1993) 6316.
[8] H.N. Chapman, A. Rode, K.A. Nugent, S.W. Wilkins, Appl. Opt. 32 (1993) 6333.
[9] P. Dhez, P. Chevallier, T.B. Lucatorto, C. Tarrio, Rev. Sci. Instrum. 70 (1999) 1907.
[10] A. Snigirev, Rev. Sci. Instrum. 66 (1995) 2053.
[11] C. David, A. Souvorov, Rev. Sci. Instrum. 70 (1999) 4168.
[12] A. Snigirev, V. Kohn, I. Snigireva, B. Lengeler, Nature 364 (1996) 49.
[13] Y.S. Park, Y.K. Ha, S.D. Park, S.H. Han, W.H. Kim, X-ray microbeam generation with optical mirrors and lens, Korea Atomic Energy Research Institute, Report KAERI/AR-706/2004.
[14] Y.S. Park, Y.K. Ha, S.D. Park, S.H. Han, K.Y. Jee, W.H. Kim, in: Proceedings of Autumn Meeting of the Korean Radioactive Waste Society, December 10–12, Jeju, Korea, PW3 25, 2004.
[15] Y.K. Ha, S.H. Han, S.D. Park, Y.S. Park, W.H. Kim, Chemical interaction between UO_2 fuel and Zircaloy clad, Korea Atomic Energy Research Institute, Report KAERI/AR-697/2004.
[16] J.H. Baek, K.B. Park, Y.H. Jeong, J. Nucl. Mater. 335 (2004) 443.
[17] T. Arima, K. Moriyama, N. Gaja, H. Furuya, K. Idemitsu, Y. Inagaki, J. Nucl. Mater. 257 (1998) 67.
[18] J.H. Kim, M.H. Lee, B.K. Choi, Y.H. Jeong, Nucl. Eng. Des. 235 (2005) 67.
[19] M. Tupin, M. Pijolat, F. Valdivieso, M. Soustelle, A. Frichet, P. Barberis, J. Nucl. Mater. 317 (2003) 130.
[20] P. Hofmann, J. Nucl. Mater. 270 (1999) 194.
[21] T.K. Kim, B.S. Choi, Y.H. Jeong, D.J. Lee, M.H. Chang, J. Nucl. Mater. 301 (2002) 81.
[22] Z. Xiaotao, W. Zhiguo, F. Xiangdong, A. Yongzhong, L. Libin, H. Xingquan, L. Yanling, Surf. Coat. Technol. 140 (2001) 161.
[23] Z. Xiaotao, F. Xiangdong, W. Zhiguo, Z. Guangting, L. Libin, L. Yanling, H. Xingquan, Surf. Coat. Technol. 148 (2001) 216.
[24] Z.G. Wang, X.T. Zu, J. Lian, X.Q. Huang, L. Wang, Y.Z. Liu, S.M. Wang, J. Alloys. Compd. 384 (2004) 93.
[25] H. Güleryüz, H. Çimenoğlu, Biomaterials 25 (2004) 3325.
[26] E.H.P. Cordfunke, R.J.M. Konings, Thermochemical Data for Reactor Materials and Fission Products, North-Holland, Amsterdam, 1990.
[27] T. Tsuji, J. Nucl. Mater. 247 (1997) 63.
[28] C.C. Ting, S.Y. Chen, D.M. Liu, Thin Solid Films 402 (2002) 290.
[29] R. Padma, K. Ramkumar, M. Satyam, J. Mater. Sci. 23 (1988) 1591.